

TARGET VALIDATION OF CYTOCHROME P450 CYP1B1 IN PROSTATE CARCINOMA WITH PROTEIN EXPRESSION IN ASSOCIATED HYPERPLASTIC AND PREMALIGNANT TISSUE

DAWN M. CARNELL, F.R.C.R.,*† ROWENA E. SMITH, M.R.C.PATH.,‡ FRANCES M. DALEY, M.Sc.,†
PAUL R. BARBER, Ph.D.,† PETER J. HOSKIN, M.D., F.R.C.R.,* GEORGE D. WILSON, Ph.D.,§
GRAEME I. MURRAY, Ph.D.,|| AND STEVEN A. EVERETT, D.Phil.†

*Marie Curie Research Wing, †Gray Cancer Institute, and ‡Department of Histopathology, Mount Vernon Hospital, Northwood, Middlesex, United Kingdom; §Karmanos Cancer Institute, Wayne State University, Detroit, MI; ||Department of Pathology, University of Aberdeen, Aberdeen, United Kingdom

Purpose: To investigate the localization and distribution of cytochrome P450 CYP1B1 protein expression in patients diagnosed with prostate carcinoma compared to those with bladder carcinoma. To validate CYP1B1 as a molecular target for the development of selective cancer therapeutics for use in combination with radiation. **Methods and Materials:** Prostatectomy specimens ($n = 33$) of moderate Gleason grade (3 + 3 and 3 + 4) were analyzed immunohistochemically for CYP1B1 protein expression using a specific monoclonal antibody for the enzyme. The intensity of CYP1B1 staining was assessed both semiquantitatively using visual scoring and quantitatively by spectral imaging microscopy using reference spectra and compared with bladder carcinoma ($n = 22$).

Results: CYP1B1 protein expression was present in 75% of prostate carcinomas ($n = 27$) compared to 100% of bladder carcinomas ($n = 22$). In both cases, CYP1B1 protein expression was heterogeneous and localized in the cytoplasm of the tumor cells but absent from the surrounding stromal tissue. CYP1B1 was also detected in premalignant prostatic intraepithelial neoplasia ($n = 2$, 100%), as well as noncancerous tissues, including benign prostatic hyperplasia ($n = 27$, 82%), metaplastic prostatic urothelium ($n = 8$, 100%), and hyperplastic prostatic urothelium ($n = 14$, 100%). Higher CYP1B1 protein expression in bladder vs. prostate carcinoma was confirmed by their corresponding average normalized absorbances (\pm standard deviation), measured as 1.40 ± 0.44 and 0.55 ± 0.09 , respectively. Overall CYP1B1 staining intensity in prostate carcinoma was similar to that in prostatic intraepithelial neoplasia, benign prostatic hyperplasia, and hyper-/metaplastic urothelial tissue. No CYP1B1 was detected in normal prostate tissue.

Conclusions: CYP1B1 is overexpressed in prostate carcinoma at a high frequency and is also detectable in the associated premalignant and hyperplastic tissue, implicating a possible link with malignant progression and CYP1B1 as a suitable target for therapy. Spectral imaging microscopy has highlighted differences in CYP1B1 protein expression between different cancers. © 2004 Elsevier Inc.

Cytochrome P450 CYP1B1, Prostate carcinoma, Bladder carcinoma, Radiation, Hyperplasia, PIN, Spectral imaging microscopy.

INTRODUCTION

Prostate cancer is the third most common cancer in men in the world, and in the majority of developed and developing countries, it is the most commonly diagnosed neoplasm affecting men beyond middle age (1). Prostate cancer is present in its preclinical form in men as young as 30, growing slowly but remaining latent for up to two decades before developing into aggressive malignant clinical cancers. There has been a global increase in the

incidence of prostatic cancer, primarily as a result of earlier diagnosis through increased availability of prostate-specific antigen (PSA) testing during the early to mid-1990s (2). The options for treatment of localized prostate carcinoma include radiotherapy (external beam radiotherapy, brachytherapy, or both), surgery (radical prostatectomy), and adjuvant hormonal treatment (3). Once locally advanced or recurrent prostate cancer becomes resistant to hormonal modulation, treatment options are severely limited, and prognosis is dismal (4).

Reprint requests to: Dr. Steven A. Everett, D. Phil., Gray Cancer Institute, P.O. Box 100, Mount Vernon Hospital, Northwood, Middlesex HA6 2JR, United Kingdom. Tel: (+44) 1923-828-611; Fax: (+44) 1923-835-210; E-mail: Everett@gci.ac.uk

Presented at ICTR 2003, Lugano, Switzerland, March 16–19,

2003.

This work is supported by the Gray Laboratory Cancer Research Trust, Mount Vernon and Watford Hospitals, and Cancer Research UK.

Received Sep 8, 2003. Accepted for publication Sep 15, 2003.

The identification of new targets associated with the malignant progression of cancer has heralded the development of molecular-targeted drugs for selective cancer therapy (5, 6). For example, aberrant epidermal growth factor receptor-tyrosine kinase activity in prostate cancer results in enhanced tumor cell proliferation and invasion and the promotion of angiogenesis. The epidermal growth factor receptor-tyrosine kinase inhibitor ZD1839 (Iressa) inhibits the growth of several human prostate cancer xenografts (both androgen dependent and independent) in combination with radiation, but this approach has yet to be fully assessed in a clinical context (7). Another example is imatinib mesylate (Glivec), a platelet-derived growth factor receptor inhibitor that is currently in early clinical trials for the treatment of refractory prostate cancer (8). However, there is a clear need to identify and exploit new targets associated with the malignant progression of prostate cancer, which in turn will drive the development of novel molecular-targeted drugs for use in the adjuvant setting with definitive surgery or radiation.

A recent study has shown that in prostate carcinoma, the level of hypoxia (median $Po_2 = 2.4$ mm Hg) correlates with PSA failure after radiotherapy (9, 10). It is recognized that nitric oxide is a potent hypoxic tumor cell radiosensitizer that can significantly enhance the effectiveness of tumor treatment by radiation provided it can be targeted selectively (11–13). The Gray Cancer Institute's strategy is to develop selective CYP1B1-activated prodrugs designed to target nitric oxide to prostate carcinoma as a means of improving tumor response to radiation treatment.

Cytochrome P450s are a multigene family of constitutively expressed and inducible enzymes involved in the oxidative metabolic activation and deactivation of carcinogens and cancer therapeutics (14). Cytochrome P450 CYP1B1 is a member of the *CYP1* gene family, which also includes CYP1A1 and CYP1A2 (15, 16). Using an antibody raised against a specific peptide sequence for CYP1B1, it has been demonstrated that the enzyme is overexpressed at a high frequency in a range of human malignancies, but not in the associated normal tissue (17–20). The expression of CYP1B1 has been observed also in breast tumors, but not in normal breast tissue (21, 22). By far the most comprehensive study of CYP1B1 protein expression in tumors has demonstrated CYP1B1 overexpression in both primary (including serous and mucinous carcinoma, $n = 170$, 80%) and secondary metastatic (secondary ovarian carcinoma, $n = 48$, 80%) ovarian cancer (23). CYP1B1 has been heralded as a new target for cancer chemotherapeutics, because of this consistent overexpression of CYP1B1 protein in a broad range of cancers compared to most drug metabolizing cytochrome P450s, including CYP1A1, CYP3A4, and CYP2D6 (14). Moreover, CYP1B1 may play an important role also in anticancer drug resistance (19, 24).

A recent study has shown that CYP1B1 mRNA is consistently expressed in prostatic tumors (25). The ap-

plication of cDNA microarray technology to profile gene expression associated with prostate tumorigenesis has shown differential gene expression of CYP1B1 between malignant and normal tissue (26). CYP1B1 mRNA has also been detected in benign prostatic hyperplasia (BPH), and CYP1 enzymes are capable of metabolic activation of compounds suspected of being prostate carcinogens (27). Although normal tissues are capable of expressing CYP1B1, the detection of CYP1B1 mRNA does not necessarily result in the concomitant CYP1B1 protein expression. For example, CYP1B1 mRNA is expressed in human liver, and the levels are increased in smokers, but the CYP1B1 protein is undetectable (28). Nevertheless, CYP1B1 protein has been detected in normal prostate tissue, albeit for a small sample size (29).

This prospective study focuses on the "profiling" of CYP1B1 protein expression in prostatic cancer to ascertain the localization and distribution of the enzyme in the carcinoma and associated premalignant and hyperplastic tissue. CYP1B1 protein expression has been detected immunohistochemically using a selective monoclonal antibody for CYP1B1, and staining intensity in the prostate tissue has been compared retrospectively to that of bladder carcinoma, where CYP1B1 protein is known to be overexpressed (20). As well as the standard semiquantitative approach, this work also exploits spectral imaging microscopy to quantify CYP1B1 staining intensity. This has enabled direct comparisons of both intra- and inter-patient CYP1B1 protein expression in prostate tissue and between different clinical tumors.

METHODS AND MATERIALS

Patient population

Informed consent was obtained from 33 patients undergoing radical prostatectomy for localized prostate carcinoma (Stage T1cN0M0–T3bN0M0, UICC 1997) at Mount Vernon and Watford hospitals. The median age was 62 years (range: 49–75 years), and the median presenting PSA was 6.7 (range: 3.53–39.1). Informed consent was obtained also from 22 patients undergoing definitive transurethral resection of transitional cell carcinoma of the bladder. The median age of patients was 68 years.

Histologic assessment of prostate and bladder tissue samples

Operative specimens were initially fixed in 10% neutral buffered formalin for 24 hours at room temperature before being embedded in paraffin wax before histopathologic analysis. Sequential sections from each block were cut to 4 μ m, mounted on coated slides (Surgipath Europ Limited, Peterborough, UK), and examined by light microscopy. Histopathologic diagnosis of hematoxylin and eosin (H&E) stained sections was made by an experienced urologic histopathologist (R.E.S.) using established histopathologic criteria. The Gleason system,

based on glandular differentiation, was used to assess the grading of prostate carcinoma (30). The majority of samples were of moderate Gleason grade (3 + 4, 17 patients; and 3 + 3, 11 patients). Three patients were scored as 2 + 3 (low grade) and 2 as high grade (4 + 4). Differentiation of benign from malignant glands was confirmed using cytokeratin 5/6 (CK5/6) staining of the basal cell layer, based on a literature method (31). The majority of bladder tumors were moderate to high grade (Grade 2: 10, Grade 3: 10), and the remaining were low grade. Sections were initially dewaxed in xylene and rehydrated through graded alcohols into water. Endogenous peroxidase was blocked using peroxidase (Dako, Denmark House, Angel Drove, Ely, Cambridgeshire, UK) for 5 min. Sections were then washed well in running tap water. A plastic trough containing 250 mL of 10-mM citric acid was prepared, and the pH was adjusted to 6.0 using 2 M sodium hydroxide. Sections were then placed into the trough, covered, and then microwaved on high power (850 W microwave) for 3 × 5-min intervals, with lost volume replaced as required. The slides were then left to stand for 10 min at room temperature. Sections were washed in water for 5 min and then rinsed in Tris-buffered saline. All sections were transferred to an automated immunostainer (Dako Autostainer S3400), and a routine program was run using Dako ChemMate reagents and CK5/6 antibody (Dako) diluted 1:300 in Tris-buffered saline. This consisted of serial incubations of 30 min each with CK5/6 primary antibody, biotinylated secondary antibody, and then the tertiary reagent (Dako ChemMate HRP kit K5001). The antigen-antibody immunoreaction was visualized using 3,3'-diaminobenzidine (ChemMate DAB). Slides were then washed well in running tap water and counterstained with Mayer's hematoxylin for 10–60 s. Sections were then dehydrated in increasing concentrations of alcohol, cleared, and mounted in DPX.

Immunohistochemical detection of CYP1B1 protein expression

The localization and distribution of CYP1B1 protein expression in prostate tissue and bladder carcinoma were determined immunohistochemically using a well-characterized monoclonal antibody selective for CYP1B1. This antibody was produced using an immunogen, a synthetic peptide corresponding to amino acids 437 and 451 of the human amino acid sequence (18). Slides were prepared for immunostaining as described above, except that the microwave time was 5 × 4-min intervals. All sections were transferred to a Dako Autostainer, and a routine program was run using Dako ChemMate reagents and CYP1B1 antibody diluted 1:25 in antibody diluent (Dako S2022). This consisted of a 60-min incubation of CYP1B1 primary antibody, 30 min incubation of secondary and tertiary reagents, followed by 5 min in DAB (DAKO ChemMate HRP kit K5001). Slides were then washed well in running tap water and counterstained with

Mayer's hematoxylin for 10–60 s. Sections were then dehydrated in increasing concentrations of alcohol, cleared, and mounted in DPX. CYP1B1 immunoreactivity within tumors was assessed as either strong (3+), moderate (2+), or weak (1+) vs. a strong bladder carcinoma positive control (3+). Both bladder and prostate tissue sections were run against the same positive control to maintain consistency. A tumor was classified as negative if less than 5% of tumor cells showed positive reactivity. No immunoreactivity was observed when the primary CYP1B1 antibody was excluded from the staining protocol.

The MaxArray Human Normal Tissue Microarray (Zymed Laboratory Inc., San Francisco, CA, USA) was used to investigate CYP1B1 protein expression in normal prostate tissue.

Spectral imaging microscopy and absorbance intensity "mapping"

Each tumor was then analyzed using spectral imaging microscopy to give a quantitative assessment of staining intensity. This technology has been developed at the Gray Cancer Institute and exploits the characteristic spectra of individual stains to distinguish stained from nonstained areas, or colocalization of stains (32). The spectral imaging device uses a standard monochrome CCD camera (Type 4912, Cohu Inc., USA) with an upright microscope (Optiphot, Nikon, UK). Representative tumor fields of 760 by 570 pixels were selected for image capture with a resolution of 0.91 $\mu\text{m}/\text{pixel}$ (eye-piece magnification ×100), and spectral analysis of the entire field was carried out. The captured image was "unmixed" using reference spectra for CYP1B1 and hematoxylin. A histogram of frequency vs. normalized absorbance intensity (against reference spectra for CYP1B1 and hematoxylin stains) was used to select an optimal threshold level for segmentation, ensuring that only the areas of interest (namely those stained for CYP1B1) contribute to the measurements. This in effect excludes the normal stromal tissue, where CYP1B1 staining is undetectable. CYP1B1 staining intensity across the entire field is given as mean normalized absorbance (\pm standard deviation [SD]). All images were captured from 400 nm to 700 nm in 24-nm steps, allowing an optimal speed of analysis time of 80 s per image. The standard deviation in mean absorbance intensity for the positive control measured on different staining runs was small (SD \pm 0.05).

RESULTS

CYP1B1 protein expression in prostate and bladder carcinoma

Immunohistochemistry for CYP1B1 protein expression indicated that the enzyme is present in 75% of the 33 prostate tumors and 100% of the 22 bladder tumors analyzed. Prostate carcinoma arises from the epithelial lining of the prostatic gland. Panels A, C, and D in Fig.

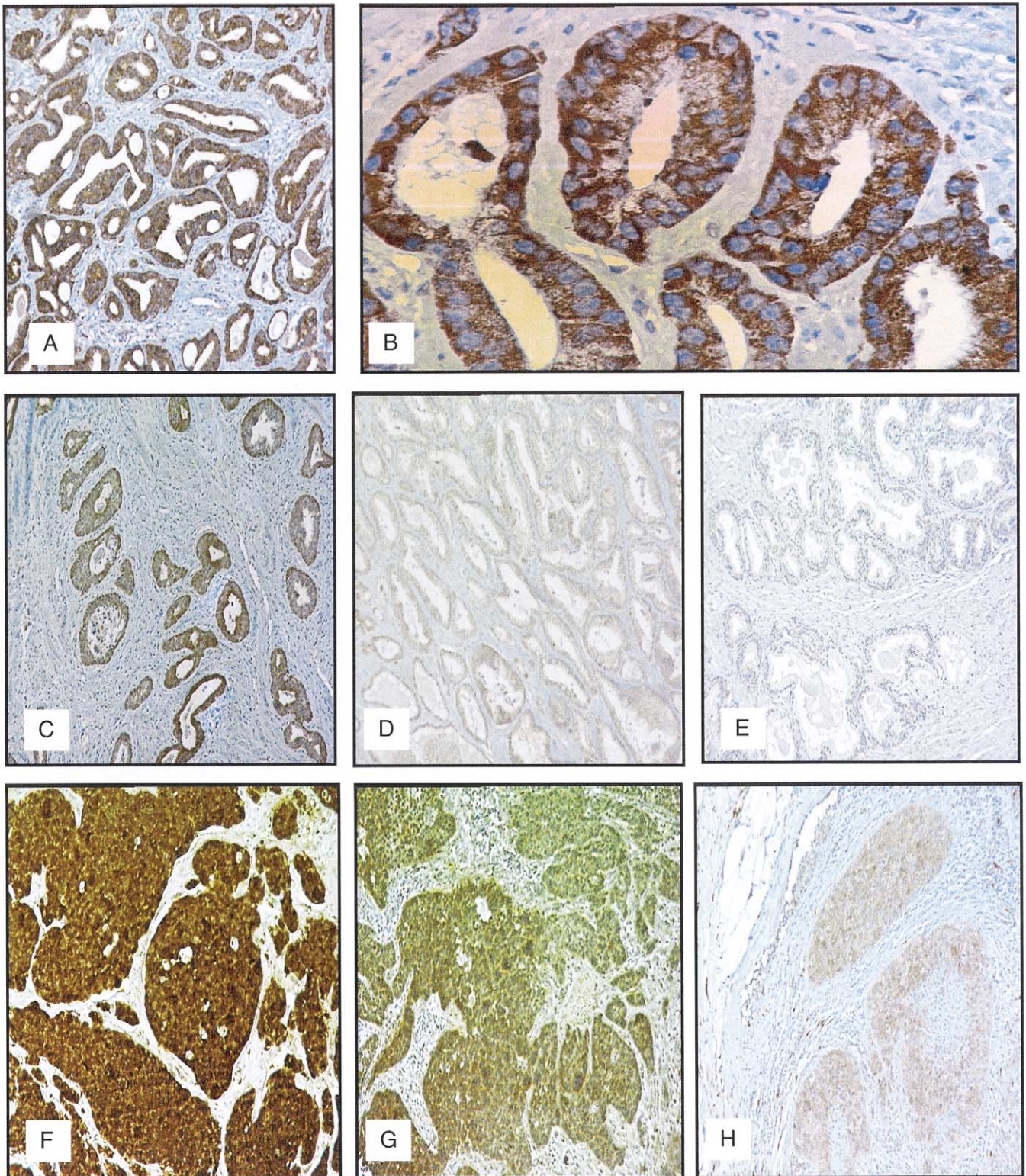


Fig. 1. Immunohistochemical detection of CYP1B1 protein expression in bladder and prostate carcinoma. (A, C, and D) Heterogeneity of CYP1B1 staining, which is absent from the supporting stromal tissue, in prostate carcinoma (magnification $\times 200$). (B) CYP1B1 is localized in the cytoplasm of the tumor cells, as exemplified by prostate carcinoma at higher magnification $\times 400$. (E) Absence of CYP1B1 in normal prostate (magnification $\times 200$). (F–H) Typify the heterogeneity of CYP1B1 protein expression in bladder carcinoma (magnification $\times 200$).

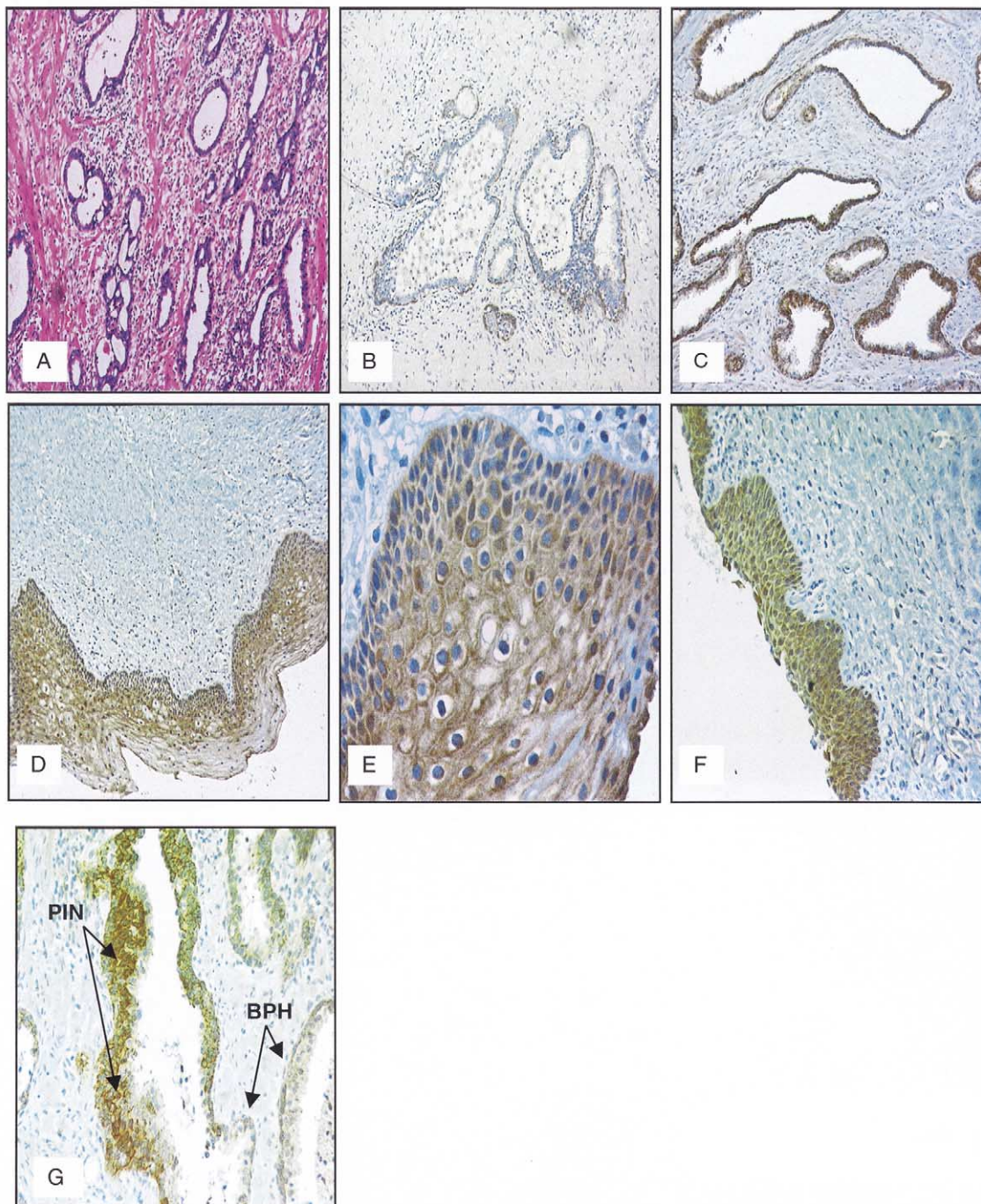


Fig. 2. Immunohistochemical detection of CYP1B1 protein expression in benign prostatic hyperplasia, hyperplastic urothelium, metaplastic urothelium, and prostatic intraepithelial neoplasia. (A–C) Confirm CYP1B1 protein expression in benign prostatic hyperplasia. (A) H&E-stained section (magnification $\times 100$) of BPH. (B) Benign glands were differentiated from malignant glands by cytokeratin 5/6 staining of the basal cells (B) (magnification $\times 200$). (C) CYP1B1 protein expression in prostate glands designated as benign (magnification $\times 200$), because they contain a basal cell layer. (D–F) Prostatic urothelium; (D and E) Squamous metaplastic changes at magnification $\times 100$ and $\times 400$, respectively. (F) An example of benign hyperplastic tissue magnification $\times 200$. (G) CYP1B1 protein expression in premalignant PIN at magnification $\times 200$. Within the same gland and adjacent gland are areas of BPH.

Table 1. CYP1B1 protein expression in bladder carcinoma and prostate carcinoma plus associated prostatic tissues

Tissue type	No. positive/no. stained	Staining intensity			Spectral imaging microscopy mean normalized absorbance \pm SD
		Visually scored			
		Strong	Moderate	Weak	
Bladder carcinoma	22/22	12 (55%)	9 (41%)	1 (4%)	1.40 \pm 0.44
Prostate carcinoma	25/33	2 (6%)	8 (24%)	15 (45%)	0.55 \pm 0.09
Prostatic intraepithelial neoplasia	2/2		2 (100%)		0.73 \pm 0.20
Metaplastic urothelium	8/8	3 (37.5%)	3 (37.5%)	2 (25%)	0.69 \pm 0.19
Hyperplastic urothelium	14/14	1 (7%)	8 (57%)	5 (36%)	0.64 \pm 0.12
Benign prostatic hyperplasia	27/33	6 (18%)	20 (61%)	1 (3%)	0.55 \pm 0.11

1 are representative sections showing the localization of CYP1B1 protein expression in glandular epithelium of moderate-grade prostate carcinoma. Figure 1B shows the subcellular localization of CYP1B1 that is present in the cytoplasm of the tumor cells. In all cases, CYP1B1 is absent from the surrounding stromal tissue. The variability of CYP1B1 staining intensity (Figs. 1A, 1C, and 1D) typifies the interpatient variability of protein expression in prostatic cancer. No CYP1B1 protein expression was detected in normal prostate tissue, as shown in Fig. 1E, in marked contrast to the overexpression of CYP1B1 in prostate carcinoma (Compare Fig. 1A and Fig. 1E).

Figure 1F and Fig. 1H show the heterogeneity of CYP1B1 protein expression in bladder carcinoma where CYP1B1 localization (present in the cytoplasm of tumor cell and absent from stroma) is similar to that of prostate carcinoma, although the tumor architecture is quite different. Table 1 shows the visual scoring of CYP1B1 staining intensity (number and frequency) for both prostate and bladder carcinoma. CYP1B1 staining intensity in bladder carcinoma was moderate to strong, in contrast to prostate carcinoma, in which staining was weak to moderate overall. The 2 patients exhibiting the strongest CYP1B1 staining are the only 2 examples of high-grade prostate carcinoma (Gleason 4 + 4). In both cases, there is a complete loss of glandular pattern with the formation of solid sheets of poorly differentiated carcinoma.

CYP1B1 protein expression in benign prostatic epithelium

Figure 2A is a representative H&E section of prostate tissue containing BPH that is characterized by a bilayer of myoepithelium. Cytokeratin 5/6 staining of the basal cell layer (Fig. 2B) was used to distinguish BPH from malignant glands. Epithelial CYP1B1 protein expression is detectable at a high frequency ($n = 27$, 82%) in BPH (Fig. 2C and Table 1) and is of mainly moderate intensity.

CYP1B1 protein expression in metaplastic and hyperplastic urothelium

Figures 2D and 2E are examples of CYP1B1 expression in metaplastic prostatic urothelium characterized by a mul-

tilayered epithelium where the cell type changes from the typical transitional cell morphology to that which is squamous in nature. In the latter case, the cells become elongated, and vacuolation is apparent more distal from the basal layer (Fig. 2E). Throughout the epithelial layer, the CYP1B1 is localized in the cytoplasm of the cells and is completely absent from the adjacent stroma. CYP1B1 was present in 100% of the 8 samples where the metaplasia was recognized and was moderate to strong in staining intensity (See Table 1).

CYP1B1 is present also in hyperplastic urothelium (Fig. 2F) that has a conserved transitional cell morphology distinct from metaplastic urothelium (Fig. 2E). CYP1B1 was detected in all cases where hyperplastic urothelium was identified ($n = 14$, 100%) and was weak to moderate in staining intensity (See Table 1).

CYP1B1 protein expression in premalignant prostatic intraepithelial neoplasia

Isolated glands containing prostatic intraepithelial neoplasia (PIN), composed of dysplastic cells with luminal cell phenotype (33), were present only in 2 of the prostate samples analyzed for CYP1B1 staining. As a consequence, it was difficult to make definitive conclusions regarding the frequency of CYP1B1 protein expression therein. Figure 2G shows CYP1B1 protein expression in PIN, and it is interesting to note that the same gland also contains BPH, which is contained also in adjacent glands in the same section (Compare Figs. 2C and 2G).

Determination of CYP1B1 staining intensity by spectral imaging microscopy

Spectral imaging microscopy was used to "map" CYP1B1 staining intensity in prostate tissue and bladder carcinoma. Figure 3A is a captured image of prostate carcinoma taken from the original tissue section, where hematoxylin in blue (Fig. 3B), is "unmixed" from CYP1B1 in brown (Fig. 3C). The absorbance intensity histogram (Fig. 3D) was generated by normalization to the individual reference spectra of hematoxylin and CYP1B1. To segment the areas of significant staining that are used to calculate an

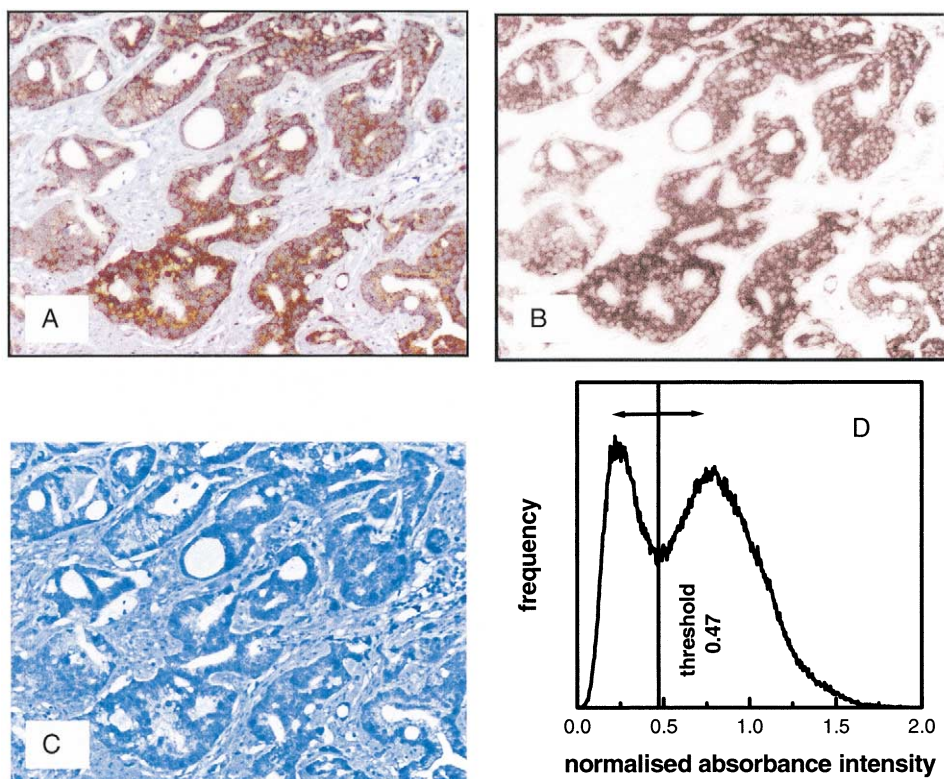


Fig. 3. Staining intensity mapping of tissue sections using spectral imaging microscopy. (A) Prostate carcinoma section stained for CYP1B1 (brown) and hematoxylin counterstain (blue) that has been spectrally unmixed and digitally separated into the component images in (B) and (C) of CYP1B1 alone and the counterstain alone, respectively. (D) Histogram of CYP1B1 staining intensity normalized to a CYP1B1 reference spectrum. A threshold of 0.47 was selected to segment the areas of intense staining that are used to calculate an average staining intensity for an image.

average staining intensity for the image, a threshold of 0.47 normalized absorbance intensity was applied to all sections. Above this threshold, absorbances are recognized as CYP1B1-specific staining; below the threshold are weak, potentially nonspecific CYP1B1 staining, plus hematoxylin staining. The threshold chosen is optimal for the segmentation of the CYP1B1 and hematoxylin spectra under the experimental conditions used for this study.

Figure 4 shows the mean normalized absorbance (\pm mean SD) for CYP1B1 staining in individual patients with (upper panel) prostate carcinoma and (lower panel) bladder carcinoma as measured by spectral imaging microscopy. In both cases, the mean standard deviation reflects the heterogeneity of CYP1B1 protein expression within the chosen field. In the case of prostate carcinoma, only 3 patients out of the 33 samples did not exhibit staining above the threshold value of 0.47 normalized absorbance intensity. This indicates that spectral imaging has detected CYP1B1 in 5 additional patients with prostate carcinoma that were previously deemed negative by standard visual scoring (See Table 1). In marked contrast, CYP1B1 was detectable in all the patients ($n = 22$) with bladder carcinoma, where CYP1B1 protein expression was significantly higher overall (range: ~ 0.47 to 2.4) than in prostate carcinoma (range: ~ 0.47 to 1.0).

Figure 5 and Table 1 show the average normalized ab-

sorbance (\pm average SD) for all the patients with bladder carcinoma and prostate carcinoma, plus the associated BPH, PIN, and metaplastic and hyperplastic urothelial tissue as measured by spectral imaging microscopy. This emphasizes that under identical staining conditions, CYP1B1 protein expression in bladder carcinoma is at least twice that in prostate carcinoma. For all the areas where CYP1B1 was detected within prostatectomy sections, the measured average normalized absorbances were fairly similar with no discernible trend.

DISCUSSION

This study has demonstrated that CYP1B1 protein is overexpressed with a high frequency in prostate carcinoma and absent from the surrounding normal stromal tissue. This observation is consistent with CYP1B1's being a tumor-related cytochrome P450 that is upregulated in a range of tumor malignancies of different histogenetic types (carcinomas, lymphomas, sarcomas, neuroepithelial tumors, and germ cell tumors) (18, 20–23, 34). However, contrary to previous immunohistochemical studies (18, 20), CYP1B1 protein expression is clearly not homogeneous in tumors with intra- and interpatient variability observed in both prostate and bladder carcinomas. Both visual scoring and spectral imaging microscopy have confirmed that CYP1B1

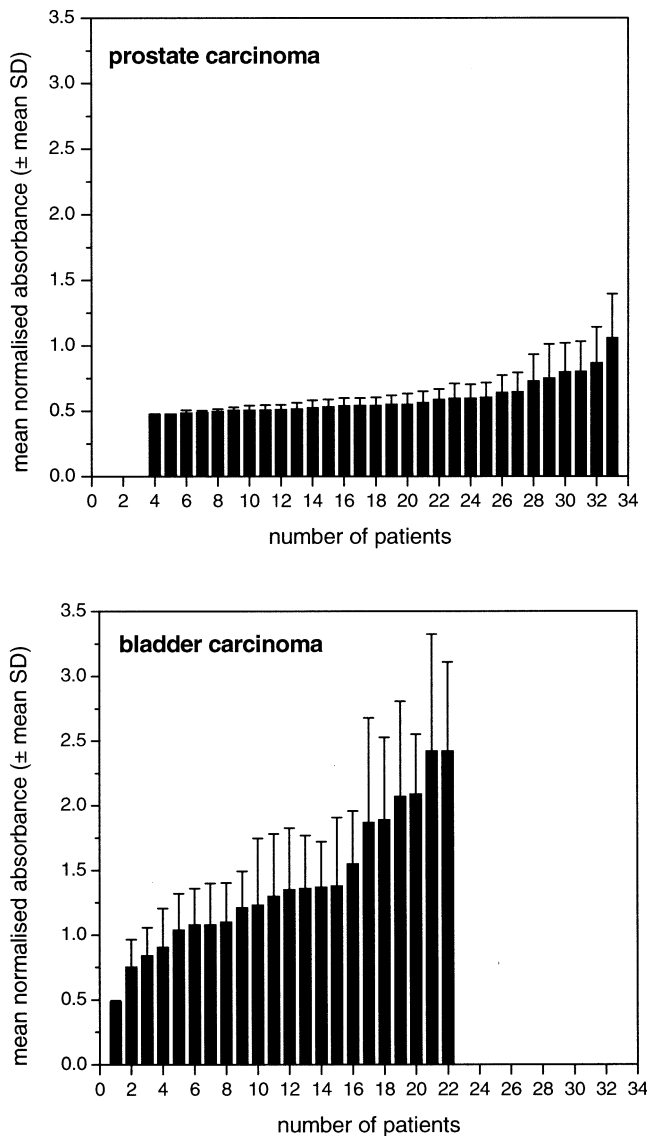


Fig. 4. The mean normalized absorbance for CYP1B1 protein expression in each individual patient with prostate carcinoma ($n = 33$) in the upper panel compared to patients with bladder carcinoma ($n = 22$) in the lower panel. In both cases, a threshold value of 0.47 was used to distinguish between sections that stained positive for CYP1B1 vs. those that were negative for CYP1B1. The mean standard deviation reflects the heterogeneity of CYP1B1 protein expression in the carcinoma tissue of individual patients.

staining intensity is stronger in bladder carcinoma than in prostate carcinoma and highlight the potential differences in CYP1B1 protein expression in clinical tumors. However, strong immunoreactivity for CYP1B1 was observed in the 2 prostate tumors of high Gleason grade (4 + 4), whereas the majority of prostate carcinomas in this study were moderately differentiated and exhibited weak to moderate immunoreactivity. No evidence was obtained for CYP1B1 expression in the nucleus (29) with protein expression present exclusively in the cytoplasm of the tumor cells.

In a recent review by Murray *et al.*, the importance of studies to examine the expression of CYP1B1 in different

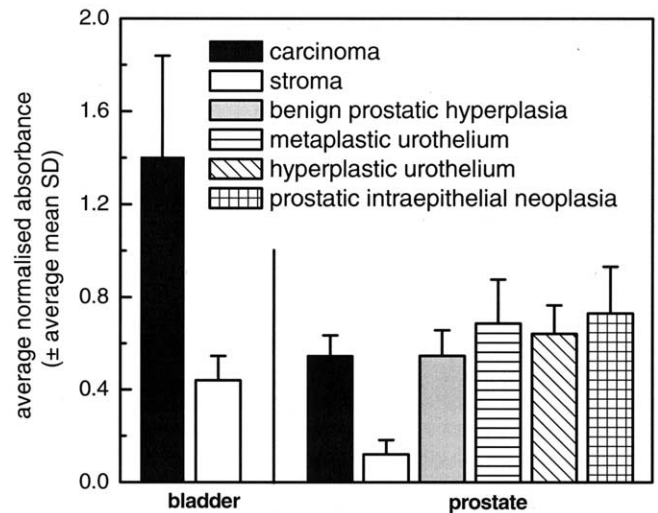


Fig. 5. A plot of the averaged normalized absorbance for all bladder carcinoma patients ($n = 22$) compared to all patients with prostate carcinoma ($n = 33$), plus associated prostatic tissue, including benign prostatic hyperplasia ($n = 27$), metaplastic urothelium ($n = 8$), hyperplastic urothelium ($n = 14$), and prostatic intraepithelial neoplasia ($n = 2$).

types of benign tumor was recognized, to identify at what stage during tumor development and progression alterations in CYP1B1 expression actually occur (16). An important observation from this work is that not only is CYP1B1 present in prostate carcinoma, but it is also expressed at a high frequency in the associated prostatic tissues, including PIN and BPH. It is recognized that PIN is the most likely precursor of invasive carcinoma of the prostate (35, 36). PIN is characterized by progressive abnormalities of phenotype that are intermediate between normal prostatic epithelium and cancer, but the exact origin of PIN (33) and whether it is derived from BPH remain unresolved. CYP1B1 protein expression has been detected in PIN, suggesting that the enzyme is expressed during premalignancy and is upregulated at an early stage of carcinogenesis. However, PIN was only present in large areas in 2 of the 33 prostatectomy specimens analyzed, which may reflect the possibility that the moderately differentiated prostate carcinoma may have overgrown the areas once occupied by PIN (37). This conclusion is supported by the fact that PIN was present in areas with a high density of BPH. In some instances, individual prostate glands appear to contain both PIN and benign epithelium, and both these neoplastic and normal/hyperplastic phenotypes express CYP1B1 protein. The detection of CYP1B1 protein expression in BPH corroborates a previous study where CYP1B1 mRNA was detected in the same tissue type (27). Whether BPH is a precursor to PIN and subsequently to carcinoma is unclear, because the various stages of malignant progression to prostate carcinoma remain to be fully resolved. However, BPH contains functional CYP1 family proteins, including CYP1A1 and CYP1B1, which are capable of metabolically activating compounds suspected of being prostate carcino-

gens (27). CYP1B1 protein expression was detected also in hyperplastic prostatic urothelium and metaplastic prostatic urothelium; the latter could be a premalignant stage of transitional cell carcinoma.

Spectral imaging microscopy has proven to be a useful technique, providing quantitative information on the CYP1B1 staining intensity in clinical tumors (32). The ability to segment and quantify overlapping stains will provide a useful means to study the potential colocalization of CYP1B1 with other biomarkers for prostatic cancer, as

well as support future investigations aimed at identifying the tumor microenvironmental factors that cause the overexpression of CYP1B1 in so many malignancies.

In conclusion, this study has demonstrated that CYP1B1 is overexpressed not only in prostate carcinoma but also in premalignant prostatic intraepithelial neoplasia and benign prostatic hyperplasia. Should this expression pattern reflect the malignant progression of prostatic cancer, CYP1B1 may prove to be an excellent target for cancer chemotherapeutics, including biologic modifiers of radiation response.

REFERENCES

- Stewart BW, Kleihues P. World Cancer Report. Lyon: IACR Press, International Agency for Research on Cancer (IACR) and the World Health Organization (WHO), 2003.
- Quinn M, Babb P. Patterns and trends in prostate cancer incidence, survival, prevalence and mortality. Part I: international comparisons. *BJU Int* 2002;90:162–173.
- Jani AB, Hellman S. Early prostate cancer: Clinical decision-making. *Lancet* 2003;361:1045–1053.
- Anonymous. A second chance for prostate-cancer chemotherapy? *Lancet Oncol* 2003;4:131.
- Workman P. Overview: Changing times: Developing cancer drugs in genomeland. *Curr Opin Investig Drugs* 2001;2:1128–1135.
- Workman P, Kaye SB. Translating basic cancer research into new cancer therapeutics. *Trends Mol Med* 2002;8:S1–9.
- Schiller JH. New directions for ZD1839 in the treatment of solid tumors. *Semin Oncol* 2003;30:49–55.
- Ko YJ, Small EJ, Kabbinavar F, et al. A multi-institutional phase II study of SU101, a platelet-derived growth factor receptor inhibitor, for patients with hormone-refractory prostate cancer. *Clin Cancer Res* 2001;7:800–805.
- Movsas B, Chapman JD, Hanlon AL, et al. Hypoxia in human prostate carcinoma: An Eppendorf PO2 study. *Am J Clin Oncol* 2001;24:458–461.
- Movsas B, Chapman JD, Hanlon AL, et al. Hypoxic prostate/muscle pO2 ratio predicts for biochemical failure in patients with prostate cancer: Preliminary findings. *Urology* 2002;60:634–639.
- Gray LH, Green FO, Hawes CA. Effect of nitric oxide on the radiosensitivity of tumour cells. *Nature* 1958;182:952–953.
- Mitchell JB, Wink DA, DeGraff W, Gamson J, Keefer LK, Krishna MC. Hypoxic mammalian cell radiosensitization by nitric oxide. *Cancer Res* 1993;53:5845–5848.
- Worthington J, Robson T, O'Keefe M, Hirst DG. Tumour cell radiosensitization using constitutive (CMV) and radiation inducible (WAF1) promoters to drive the iNOS gene: A novel suicide gene therapy. *Gene Ther* 2002;9:263–269.
- Patterson LH, Murray GI. Tumour cytochrome P450 and drug activation. *Curr Pharm Des* 2002;8:1335–1347.
- Sutter TR, Tang YM, Hayes CL, et al. Complete cDNA sequence of a human dioxin-inducible mRNA identifies a new gene subfamily of cytochrome P450 that maps to chromosome 2. *J Biol Chem* 1994;269:13092–13099.
- Murray GI, Melvin WT, Greenlee WF, Burke MD. Regulation, function, and tissue-specific expression of cytochrome P450 CYP1B1. *Annu Rev Pharmacol Toxicol* 2001;41:297–316.
- Cheung YL, Kerr AC, McFadyen MC, Melvin WT, Murray GI. Differential expression of CYP1A1, CYP1A2, CYP1B1 in human kidney tumours. *Cancer Lett* 1999;139:199–205.
- McFadyen MC, Breeman S, Payne S, et al. Immunohistochemical localization of cytochrome P450 CYP1B1 in breast cancer with monoclonal antibodies specific for CYP1B1. *J Histochem Cytochem* 1999;47:1457–1464.
- McFadyen MC, McLeod HL, Jackson FC, Melvin WT, Doehmer J, Murray GI. Cytochrome P450 CYP1B1 protein expression: A novel mechanism of anticancer drug resistance. *Biochem Pharmacol* 2001;62:207–212.
- Murray GI, Taylor MC, McFadyen MC, et al. Tumor-specific expression of cytochrome P450 CYP1B1. *Cancer Res* 1997;57:3026–3031.
- Huang Z, Fasco MJ, Figge HL, Keyomarsi K, Kaminsky LS. Expression of cytochromes P450 in human breast tissue and tumors. *Drug Metab Dispos* 1996;24:899–905.
- Kaminsky LS, Spivack SD. Cytochromes P450 and cancer. *Mol Aspects Med* 1999;20:70, 84–137.
- McFadyen MC, Cruickshank ME, Miller ID, et al. Cytochrome P450 CYP1B1 over-expression in primary and metastatic ovarian cancer. *Br J Cancer* 2001;85:242–246.
- Rochat B, Morsman JM, Murray GI, Figg WD, McLeod HL. Human CYP1B1 and anticancer agent metabolism: Mechanism for tumor-specific drug inactivation? *J Pharmacol Exp Ther* 2001;296:537–541.
- Finnstrom N, Bjelfman C, Soderstrom TG, et al. Detection of cytochrome P450 mRNA transcripts in prostate samples by RT-PCR. *Eur J Clin Invest* 2001;31:880–886.
- Chaib H, Cockrell EK, Rubin MA, Macoska JA. Profiling and verification of gene expression patterns in normal and malignant human prostate tissues by cDNA microarray analysis. *Neoplasia* 2001;3:43–52.
- Williams JA, Martin FL, Muir GH, Hewer A, Grover PL, Phillips DH. Metabolic activation of carcinogens and expression of various cytochromes P450 in human prostate tissue. *Carcinogenesis* 2000;21:1683–1689.
- Chang TK, Chen J, Pillay V, Ho JY, Bandiera SM. Real-time polymerase chain reaction analysis of CYP1B1 gene expression in human liver. *Toxicol Sci* 2003;71:11–19.
- Muskhelishvili L, Thompson PA, Kusewitt DF, Wang C, Kadlubar FF. In situ hybridization and immunohistochemical analysis of cytochrome P450 1B1 expression in human normal tissues. *J Histochem Cytochem* 2001;49:229–236.
- Gleason DF. Histologic grading of prostate cancer: A perspective. *Hum Pathol* 1992;23:273–279.
- Abrahams NA, Ormsby AH, Brainard J. Validation of cytokeratin 5/6 as an effective substitute for keratin 903 in the differentiation of benign from malignant glands in prostate needle biopsies. *Histopathology* 2002;41:35–41.
- Barber PR, Vojnovic B, Atkin G, et al. Applications of cost-effective spectral imaging microscopy in cancer research. *J Phys D: Appl Phys* 2003;36:1729–1738.
- Montironi R, Mazzucchelli R, Scarpelli M. Precancerous lesions and conditions of the prostate: From morphological and biological characterization to chemoprevention. *Ann NY Acad Sci* 2002;963:169–184.

34. Murray GI. The role of cytochrome P450 in tumour development and progression and its potential in therapy. *J Pathol* 2000;192:419–426.
35. Feneley MR, Green JS, Young MP, *et al.* Prevalence of prostatic intra-epithelial neoplasia (PIN) in biopsies from hospital practice and pilot screening: Clinical implications. *Prostate Cancer Prostatic Dis* 1997;1:79–83.
36. Woderich R, McLoughlin J, Deen S. Radical prostatectomy for high grade prostatic intraepithelial neoplasia. *Int Urol Nephrol* 2001;33:649–650.
37. Green JS, Knight RJ, Hunter-Campbell P, *et al.* An investigation into the spatial relationship between prostate intraepithelial neoplasia and cancer. *Prostate Cancer Prostatic Dis* 2001;4:97–100.